Cis and trans modifiers in facioscapulohumeral muscular dystrophy

Sikrová, D.

CHAPTER 5

Lrif1 is required for Trim28-mediated repression of *Dux* in mouse embryonic stem cells

Darina Šikrová[1], Román González-Prieto[2], Alfred C. O. Vertegaal[2], Judit Balog[1], Lucia Daxinger[1] and Silvère M. van der Maarel[1]

[1]Department of Human Genetics, Leiden University Medical Center, 2333ZC Leiden, The Netherlands
[2]Department of Cell and Chemical Biology, Leiden University Medical Center, Leiden, The Netherlands

Manuscript in preparation

Abstract

Germline mutations in *SMCHD1*, *DNMT3B* and *LRIF1* can cause Facioscapulohumeral muscular dystrophy type 2 (FSHD2). FSHD is an epigenetic skeletal muscle disorder in which incomplete heterochromatinization of the D4Z4 macrosatellite repeat causes spurious expression of the repeat-embedded *DUX4* gene in skeletal muscle, ultimately leading to muscle weakness and wasting. All three proteins play a role in chromatin organization and gene silencing, however, a potential direct functional interplay has not been elucidated yet. Here, we show that siRNA-mediated depletion of Lrif1, but not of the other two FSHD2 genes, in mouse embryonic stem cells leads to upregulation of the 2-cell cleavage stage transcriptional program driven by the transcription factor Dux, which is the mouse functional homologue of human DUX4. Furthermore, we show that Lrif1 interacts with Trim28, a known *Dux* repressor, and that this interaction is independent of Cbx proteins and Smchd1. We uncover that *Dux* upregulation in Lrif1 knock-down mESCs is due to decreased Trim28 occupancy at the *Dux* locus itself. Together, our results provide evidence for a conserved function of Lrif1 in repressing the expression of an early zygotic genome activator both in mouse and human.

Main

To test the potential functional cooperation among FSHD2 gene products, we made use of serum/LIF-cultured E14 mESCs in which the expression of all three FSHD2 genes physiologically coincides, and performed siRNA-mediated knock down of each disease gene product followed by total RNA-seq. In contrast to the *Smchd1* gene, for which only one mRNA isoform is expressed in this culture system, *Dnmt3b* and *Lrif1* genes give rise to at least three different protein-coding isoforms in E14 mESCs (Figure 1A). Interestingly, only two protein-coding isoforms are annotated for human *LRIF1* (referred to as long and short) whereas in mouse a third isoform is produced by an alternative upstream transcriptional start site (Suppl. Figure 1A). This isoform contains an N-terminal extension of 16 aa to the short Lrif1 isoform (Figure 1A). Thus, to ensure targeting of all isoforms, we used a mix of four siRNAs for each gene. Cells were harvested after two consecutive two days-long knock-downs, which resulted in efficient protein (Figure 1A) and mRNA (Figure 1B) depletion, while mRNA and protein levels of the untargeted FSHD2 genes remained unaffected (Figure 1A and 1B). The mRNA levels of three tested pluripotency markers (*Oct4*, *Nanog* and *Sox2*) were largely unaffected upon respective knock-downs, however, we detected mild but significant downregulation of *Sox2* mRNA levels upon Lrif1 knock-down (Figure 1C). Together, this suggests that short-term depletion of the three FSHD2 disease proteins does not impair pluripotency in serum/LIF grown mESCs.

To better understand the roles of these factors in gene regulation, we first performed total RNA-seq. This revealed only subtle gene expression changes in the knock-down conditions (when considering 2-fold expression changes in either direction) as compared to the control condition. The Lrif1 knock-down condition showed the highest number of differentially expressed genes (749 DEGs with p.adj. <0.05), the majority of which were of modest fold changes (Figure 1D). Next, we assessed whether differentially expressed genes were shared between the different knock downs. Despite statistically significant overlaps between differentially upregulated and downregulated genes in paired comparisons of the knock-down conditions, only a limited number of upregulated and downregulated genes (23 and 9, respectively) was common among all three knock-down conditions (Figure 1G and 1H, Suppl. Table 1). This limited overlap prohibits pathway analysis and suggests rather divergent effects of these proteins on the transcriptome in mESCs.

Interestingly, the top differentially upregulated genes in Lrif1 knock-down mESCs (such as the *Zscan4* cluster genes) belong to a class of genes that is specifically expressed at the two cell (2C) cleavage stage of the mouse embryo[1–4] (Figure 1D). The 2C-like cells spontaneously arise in mESC culture accounting for less than 1% of the population[3] and they mimic some of the distinctive features of the 2C-stage embryos (reviewed here[5]). Furthermore, expression analysis of repetitive elements in Lrif1 knock-down mESCs showed a significant increase in transcripts originating from repeats, which are known to be de-repressed in the 2-cell embryo as well as in the 2C-like mESCs population, such as major satellites and MERVL elements (Suppl. Figure 1B).

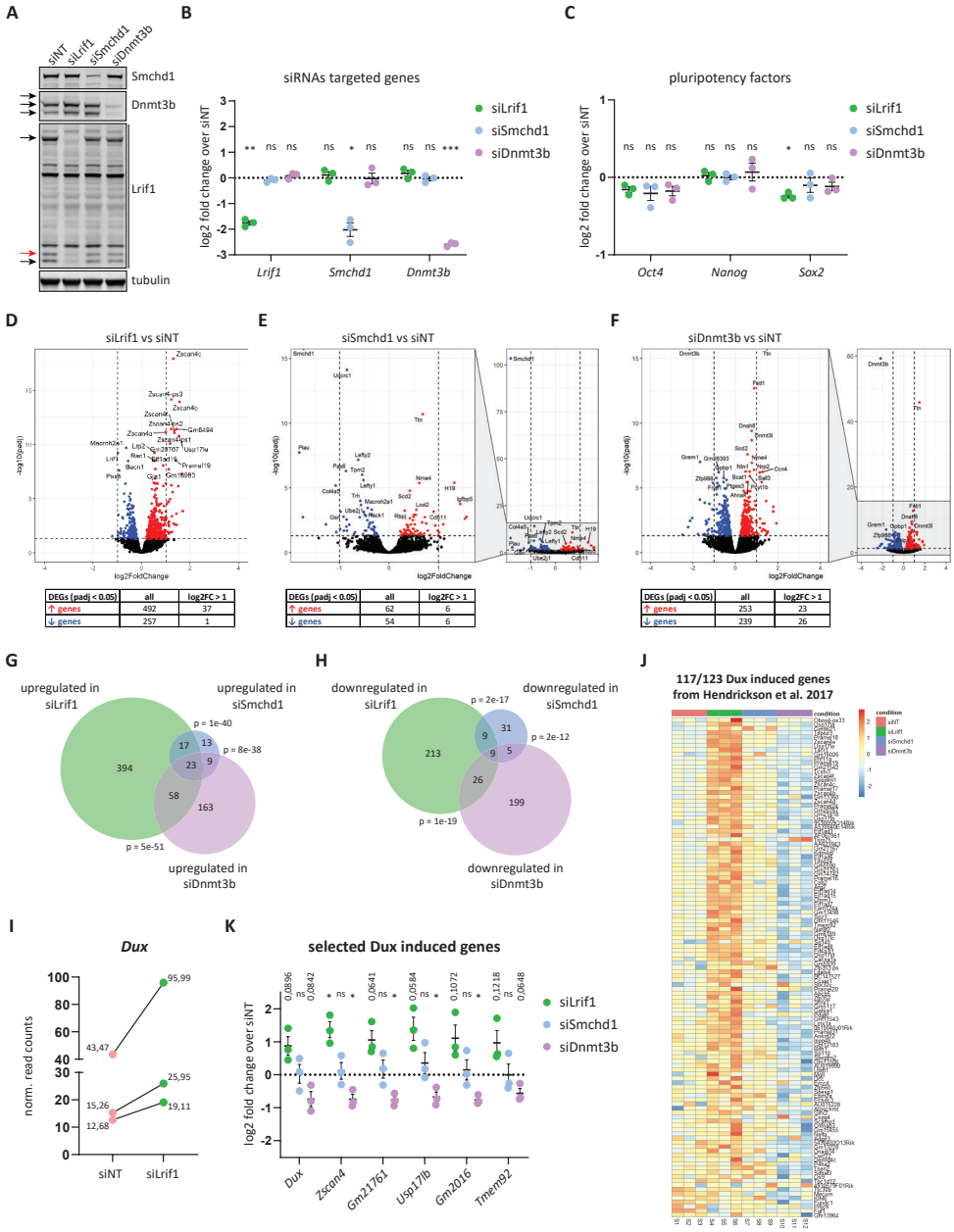

Figure 1. Lrif1 knock-down causes upregulation of Dux sensitive genes. A) Western blot confirmation of successful siRNA-mediated knock-down of three FSHD2 genes (Lrif1, Smchd1 and Dnmt3b) in E14 mESCs. Arrows mark different protein isoforms of Dnmt3b and Lrif1. The red arrow marks extra mouse-specific Lrif1 isoform not identified in human. Tubulin served as loading control. **B)** RT-qPCR confirmation of downregulation of three FSHD2 genes after siRNA-mediated knock-down in E14 mESCs. Expression levels detected in knock-down conditions were normalized to the siNT condition and log2 transformed. Every dot represents an independent biological replicate. Whiskers represent mean ± SEM. Statistical significance was calculate by one-sample t-test (ns: not significant, *:

< 0.05, **: < 0.01, ***: < 0.001). **C)** RT-qPCR of three pluripotency genes (*Oct4*, *Nanog* and *Sox2*) after individual siRNA-mediated knock-down of three FSHD2 genes. Expression levels in knock-down conditions were normalized to the siNT condition and log2 transformed. Every dot represents an independent biological replicate. Whiskers represent mean ± SEM. Statistical significance was calculate by one-sample t-test (ns: not significant, *: < 0.05). **D)** Volcano plot showing gene expression changes following Lrif1 knock-down. Upregulated genes are highlighted in red and downregulated genes are highlighted in blue. Dashed lines indicate a fold change of two (log_2 fold of 1) on the x axis and significance of 0.05 (−log10 p.adj of 1.3) on the y axis. Top 20 differentially expressed genes (DEGs) are labelled. Table summary of DEGs is provided below the plot. **E)** Volcano plot showing gene expression changes following Smchd1 knock-down. Upregulated genes are highlighted in red and downregulated genes are highlighted in blue. Dashed lines indicate a fold change of two (log_2 fold of 1) on the x axis and significance of 0.05 (−log10 p.adj of 1.3) on the y axis. Top 20 differentially expressed genes (DEGs) are labelled. Table summary of DEGs is provided below the plot. **F)** Volcano plot showing gene expression changes following Dnmt3b knock-down. Upregulated genes are highlighted in red and downregulated genes are highlighted in blue. Dashed lines indicate a fold change of two (log_2 fold of 1) on the x axis and significance of 0.05 (−log10 p.adj of 1.3) on the y axis. Top 20 differentially expressed genes (DEGs) are labelled. Table summary of DEGs is provided below the plot. **G)** Overlap of common significantly upregulated genes (p.adj. < 0.05) in all three knock-down conditions. The significance of overlaps was calculated with Fischer's exact test. **H)** Overlap of common significantly downregulated genes (p.adj. < 0.05) in all three knock-down conditions. The significance of overlaps was calculated with Fischer's exact test. **I)** Changes in normalized read counts of Dux transcripts after Lrif1 knock down compared to non-targeting siRNA condition. **J)** Heatmap depicting expression changes of previously reported 117 Dux-induced genes (out of 123 reported by Hendrickson et al.) in different knock-down conditions for which there was a non-zero reads count. **K)** RT-qPCR of Dux and five Dux-sensitive genes after siRNA-mediated knock-down in E14 mESCs. Expression levels detected in knock-down conditions were normalized to siNT condition and log2 transformed. Every dot represents an independent biological replicate. Whiskers represent mean ± SEM. Statistical significance was calculate by one-sample t-test (ns: not significant, *: < 0.05).

Expression of many 2C-like genes and repeats is known to be driven by the transcription factor Dux, which is the functional homologue of primate DUX4. Initially, the *Dux* gene itself was not identified as significantly differentially upregulated in Lrif1 knock-down mESCs. However, plotting the normalized read counts of *Dux* in each Lrif1 knock-down experiment individually showed a modest increase in read numbers in each knock-down experiment (Figure 1I), whereas *Dux* normalized read counts did not increase in the other two knock-down conditions (Suppl. Figure 1C and 1D). Therefore, we closely examined the expression levels of selected genes previously described by Hendrickson et al.[6], which are sensitive to Dux overexpression in mESCs (hereafter referred to as Dux signature genes). This inspection revealed that, in general, the mRNA levels of Dux signature genes increased upon Lrif1 knock-down (Figure 1J). In contrast, Dux signature genes remained unchanged in the Smchd1 knock-down situation (Figure 1J). In addition, Dnmt3b knock-down seemed to result in decreased expression of *Dux* and Dux signature genes (Suppl. Figure 1D and Figure 1J). We validated with RT-qPCR the mRNA expression of five selected Dux signature genes (*Zscan4*, *Gm21761*, *Usp17lb*, *Gm2016*, *Tmem92*) and *Dux* itself, and confirmed their upregulation in Lrif1 knock-down mESCs, albeit not always reaching statistical significance (Figure 1K). We further confirmed reduced and unaffected mRNA levels of these genes in Dnmt3b and Smchd1 knock-down mESCs, respectively (Figure 1K). Consistent with the RNA-seq, the expression changes were subtle. Therefore, these results indicate that Lrif1 confers a mild repression of the Dux driven 2C-like transcriptional program in mESCs under these experimental conditions.

Initially, treatment of mESCs with trichostatin A, an inhibitor of histone deacetylases, was shown to promote the emergence of 2C-like cells in mESC culture, which suggested that the chromatin configuration plays a role in this cellular transition[3]. Several chromatin-regulating factors have since been reported to directly influence *Dux* expression in mESCs [7–11]. We decided to investigate the protein interactome of Lrif1 in mESCs with the aim to identify potential interactors that could explain Lrif1's contribution to regulation of 2C-like cells. To this end, we generated constructs encoding two GFP-tagged Lrif1 isoforms which correspond to the amino acid sequences of the human long and short LRIF1 isoforms. Upon transient transfection of these plasmids in E14 mESCs, we performed GFP-specific pull-down followed by mass spectrometry (MS). The MS analysis identified 54 proteins enriched in GFP-Lrif1s pull-down of which 37 were nuclear (Figure 2A) and 94 proteins enriched in GFP-Lrif1l pull-down of which 44 were nuclear (Figure 2B). The full spectrum of results can be viewed in Suppl. Table 2, however, we focused our further analysis only on nuclear proteins since Lrif1 mainly localizes to this cellular compartment[12].

We found that nuclear proteins enriched in the GFP-Lrif1s pull-down largely overlapped with proteins identified in the GFP-Lrif1l pull-down (Figure 2C). Smchd1 and three Cbx paralogues were among the top four interactors, which is consistent with previous findings[13–15]. We identified Trim28 (tripartite motif-containing protein 28; also known as Kap1) as a common interacting partner of both Lrif1 isoforms Trim28 has previously been shown to be involved in direct repression of the *Dux* locus in mESCs[7,10]. In addition, several studies showed that depletion of Trim28 in mESCs cells leads to an increase in the 2C-like population in Dux-dependent manner[3,7,10]. To address a putative cooperation between Lrif1 and Trim28, we first confirmed the Trim28 interaction with both Lrif1 isoforms by repeating the transfection of GFP-tagged Lrif1 isoforms in mESCs followed by GFP-specific pull down and western blot analysis (Figure 2D). We further validated this interaction by performing reciprocal endogenous Co-IPs from mESC whole cell extract treated with benzonase to rule out possible DNA-mediated interactions using two different Trim28 antibodies and one Lrif1 antibody (Figure 2E and 2F). Detection of endogenous Lrif1s was prohibited by its co-migration in the gel with the antibody light chain that was used for Co-IP which was of the same species origin as the primary antibody used for Lrif1 detection.

Interestingly, we could also pull-down Smchd1 (Figure 2E and 2F) and Cbx3 (Figure 2F) in the Trim28 Co-IPs. Similar to Lrif1, Trim28 contains a conserved Cbx binding motif (PxVxL; where x represents any amino acid), which is essential for transcriptional silencing imposed by Trim28[16]. We speculated that the interaction between Lrif1 and Trim28 might therefore be bridged via Cbx proteins, which are the homologues of human HP1 proteins[17]. To test this hypothesis, we introduced previously characterized mutations (mPVL) in the HP1 binding motif of the human LRIF1 long isoform[15] to our GFP-tagged long and short mouse Lrif1 constructs (Figure 2G). The mPVL mutant carries two amino acid substitutions (V47D/L51E in the short isoform; V567D/L569E in the long isoform) in the conserved HP1 binding motif which abolish the interaction of LRIF1 with the chromoshadow domain of human HP1 proteins. We included in this experiment an additional previously characterized LRIF1 mutant termed m1[15].

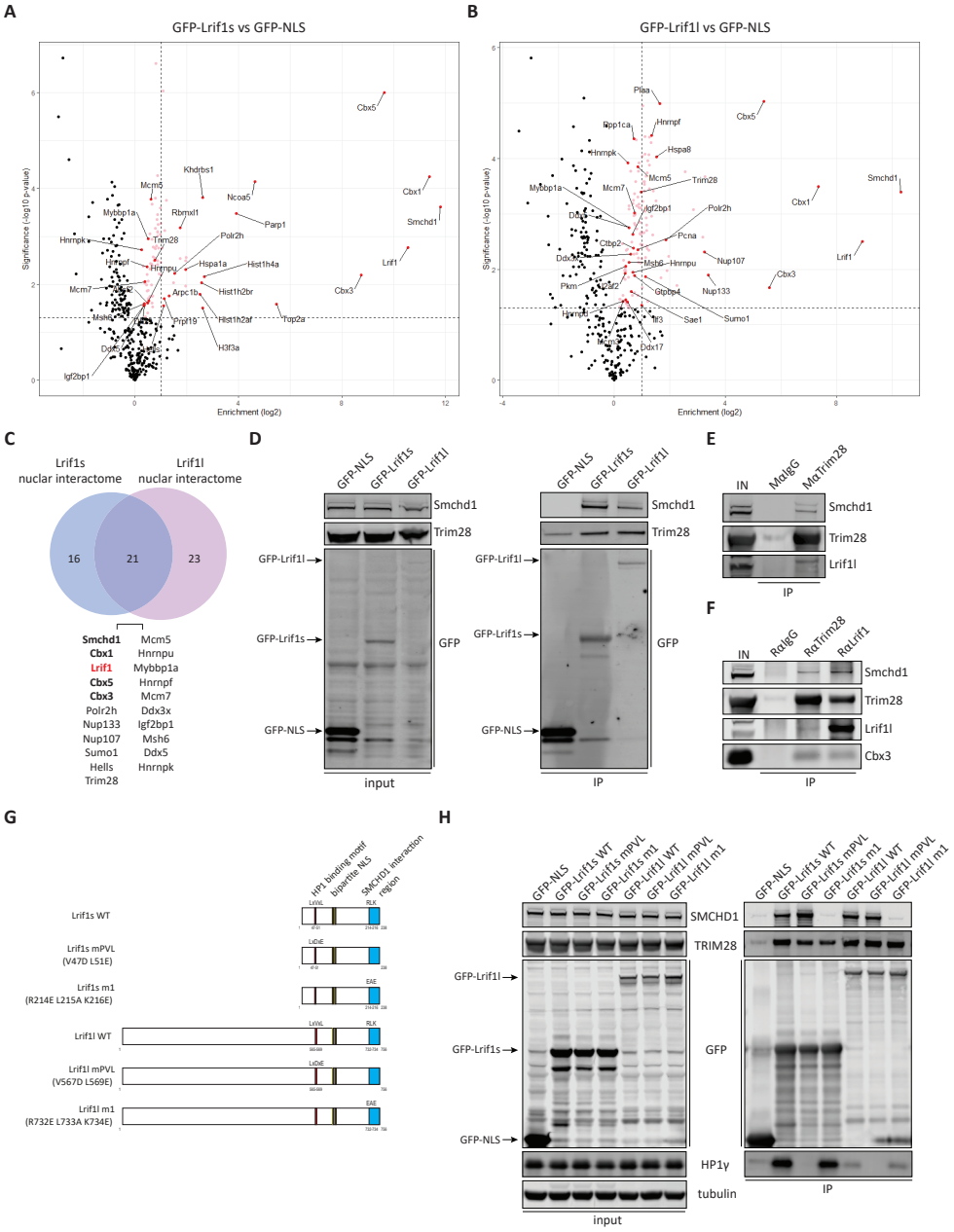

Figure 2. Lrif1 isoforms interact with Trim28. A) Volcano plot showing the differential interactome of the GFP-tagged Lrif1 short isoform over GFP-NLS as identified by GFP pull-down followed by label-free MS. GFP pull-downs were performed in biological triplicate. The enrichment (log2) is plotted on the x axis and the significance (−log10 p-value) is plotted on the y axis. The dashed line indicates a significance of 0.05 (−log10 P value of 1.3) on the y axis. Red dots mark significantly enriched nuclear proteins and pink dots mark significantly enriched non-nuclear proteins. Ribosomal proteins are not shown. All significantly enriched nuclear proteins are labelled. **B)** Volcano plot showing the differential interactome of the GFP-tagged Lrif1 long isoform over GFP-NLS. The same description applies for this plot

as for the plot in A). **C)** Venn diagram of overlapping significantly enriched nuclear proteins between GFP-tagged Lrif1 short and long isoform interactomes. **D)** Western blot confirmation of the Lrif1-Trim28 interaction by GFP pull-down of GFP-NLS, GFP-Lrif1s or GFP-Lrif1l. **E)** Endogenous MαTrim28 Co-IP on benzonase treated mESC whole cell extract. MαIgG was used as a negative control. Only the long isoform of Lrif1 is probed for as the short Lrif1 isoform protein migrates at the hight of IgG light chain. **F)** Reciprocal endogenous RαTrim28 and RαLrif1 Co-IP on benzonase treated mESC whole cell extract. MαIgG was used as a negative control. Only the long isoform of Lrif1 is probed for as the short Lrif1 isoform protein migrates at the hight of IgG light chain. **G)** Schematic representation of WT Lrif1 isoforms and their mutant forms used for GFP Co-IPs to test for TRIM28 interaction. **H)** GFP pull-downs of GFP-NLS, GFP-tagged WT and mutant Lrif1 isoforms in benzonase treated HEK293T whole cell extracts.

This mutant carries three amino acid substitutions in the C-terminal coil-coiled domain (R214/L215A/K216E in the short isoform; R732E/L733A/K734E in the long isoform) of LRIF1, which compromises the interaction with SMCHD1[15]. Since the transfection efficiency of mESCs was suboptimal for these CoIPs and there was a substantial background of Trim28 enrichment in the GFP only pull down from mESCs whole cell lysates, although with less signal than with the GFP-Lrif1 fusion proteins (Figure 2D), we performed the experiment in HEK293T cells. As anticipated due to functional motif conservation[15], both mouse Lrif1 isoforms interacted with the human SMCHD1 and CBX3/HP1$_\gamma$ proteins as well as with human TRIM28 (Figure 2H). Next, we assessed the Trim28 interaction with the mutated forms of Lrif1. As expected, the mPVL mutant abolished the interaction of Lrif1 with human HP1$_\gamma$ which corresponds with mouse Cbx3 and the m1 mutant of Lrif1 abolished the interaction with human SMCHD1. Surprisingly, neither of the mutants affected Lrif1's interaction with TRIM28 (Figure 2H). This suggests that the interaction of Lrif1 with TRIM28 is not mediated via HP1 proteins nor via SMCHD1 or its coiled-coil domain and that another region shared by both Lrif1 isoforms is responsible for this interaction.

Since Trim28 is known to repress *Dux* by directly binding to its genomic locus[7,10] and we uncovered an interaction between Lrif1 and Trim28, we were keen to investigate a potential interplay of Lrif1 and Trim28 at the *Dux* locus. First, we employed siRNA-mediated short-term depletion of either Lrif1 or Trim28 and confirmed their knock down efficiency by western blot (Figure 3A) as well as by RT-qPCR (Figure 3B). Lrif1 knock-down did not affect protein levels of Trim28 or the other two Lrif1 interacting partners (Smchd1 and Cbx3), which are also known to regulate *Dux* expression[8,18]. This result rules out the possibility that the observed increased *Dux* expression in Lrif1 knock-down is due to lower levels of any of these *Dux* repressors. A two day-long knock-down of Trim28 was already sufficient to cause mild downregulation in expression of three examined pluripotency factors (Figure 3C), which is in agreement with its essential role in pluripotency maintenance and self-renewal of mESCs cultured in serum/LIF condition[19]. Despite that, we could detect by RT-qPCR a modest upregulation of *Dux* and five of its signature genes in both knock-down situations (Figure 3D). Next, we wanted to assess if Lrif1 has a direct role in regulating the *Dux* locus by measuring Lrif1 occupancy using chromatin immunoprecipitation (ChIP). Since there is no ChIP-grade antibody for mouse Lrif1 available, we focused on a potential Lrif1-dependent Trim28 binding to the *Dux* locus. As expected, Trim28 knock-down leads to decreased Trim28 enrichment at the *Dux* locus (Figure 3E) as well as at IAPEz elements (Suppl. Figure 2A), which are also innate genomic targets of Trim28-imposed repression in mESCs[19,20].

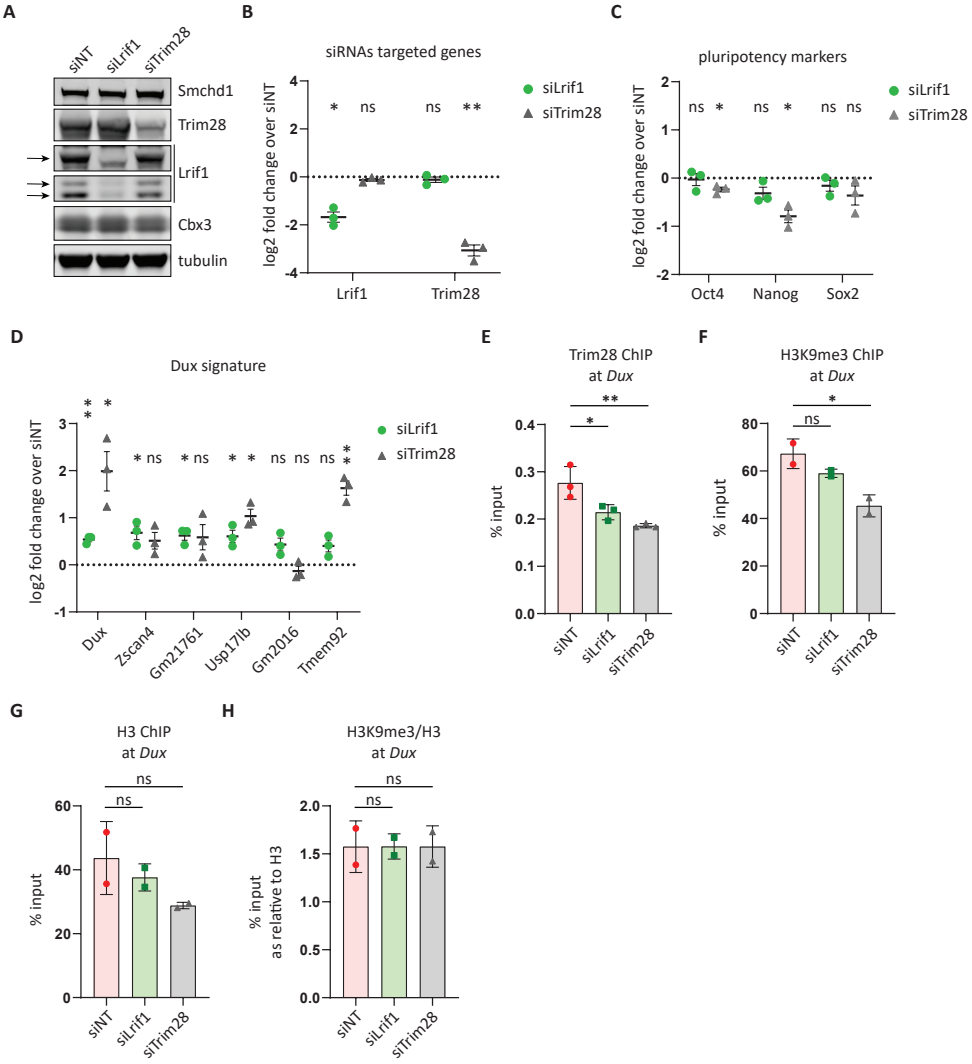

Figure 3. Trim28 requires Lrif1 for its binding to the *Dux* repeat. A) Western blot confirmation of successful siRNA-mediated knock-down of Lrif1 or Trim28 in E14 mESCs. Arrows mark different protein isoforms of Lrif1. Tubulin served as a loading control. Protein levels of two other Lrif1 interactors (Smchd1 and Cbx3) are not changed. **B)** RT-qPCR confirmation of Lrif1 and Trim28 downregulation after siRNA-mediated knock-down in E14 mESCs. Expression levels detected in knock-down conditions were normalized to the siNT condition and log2 transformed. Every dot represents an independent biological replicate. Whiskers represent mean ± SEM. Statistical significance was calculate by one-sample t-test (ns: not significant, *: < 0.05, **: < 0.01). **C)** RT-qPCR of three pluripotency genes (*Oct4*, *Nanog* and *Sox2*) after siRNA-mediated knock-down of Lrif1 or Trim28. Expression levels in knock-down conditions were normalized to the siNT condition and log2 transformed. Every dot represents an independent biological replicate. Whiskers represent mean ± SEM. Statistical significance was calculated by one-sample t-test (ns: not significant, *: < 0.05). **D)** RT-qPCR of Dux and five Dux- sensitive genes after siRNA-mediated knock-down of Lrif1 or Trim28. Expression levels in knock-down conditions were normalized to the siNT condition and log2 transformed. Every dot represents an independent biological replicate. Whiskers represent mean ± SEM. Statistical significance was calculated by one-sample t-test (ns:

not significant, *: < 0.05, **: < 0.01). **E)** Trim28 ChIP-qPCR of the 5' Dux region in E14 mESCs after treatment with respective siRNAs. Bars and whiskers represent mean ± SEM of three independent experiments. Statistical significance was calculated by one-way ANOVA with Dunnett's post hoc test (*: < 0.05, **: < 0.01). **F)** H3K9me3 ChIP-qPCR of the 5' Dux region in E14 mESCs after treatment with respective siRNAs. Bars and whiskers represent mean ± SEM of two independent experiments. Statistical significance was calculated by one-way ANOVA with Dunnett's post hoc test (ns: not significant, *: < 0.05). **G)** H3 ChIP-qPCR of the 5' Dux region in E14 mESCs after treatment with respective siRNAs. Bars and whiskers represent mean ± SEM of two independent experiments. Statistical significance was calculated by one-way ANOVA with Dunnett's post hoc test (ns: not significant). **H)** Ratio of H3K9me3 levels to H3 levels at Dux calculated from enrichment values presented in F) for H3K9me3 and G) for H3. Statistical significance was calculated by one-way ANOVA with Dunnett's post hoc test (ns: not significant).

The Trim28 signal at intron 2 of *Gapdh,* which served as negative control region*,* remained unchanged in both knock-down conditions thus representing only antibody background signal (Suppl. Figure 2B). Interestingly, Lrif1 knock-down itself resulted in reduced Trim28 enrichment at *Dux*, albeit to a lesser degree than observed in the Trim28 knock-down condition (Figure 3E). In contrast, the Trim28 enrichment at IAPez elements remained unaffected in Lrif1 knock-down mESCs (Suppl. Figure 2A). This is in agreement with our siLrif1 RNAseq data, where we did not detect increased expression from this class of repetitive elements (Suppl. Figure 1B). Together this points to an Lrif1-independent regulation of these repeats by Trim28.

Lastly, since the repressive histone modification H3K9me3 is a known canonical marker of Trim28-mediated repression[19], we measured its levels at the *Dux* locus to test if reduced Trim28 binding at this locus upon Lrif1 knock-down leads to a concomitant decrease of this modification. ChIP-qPCR showed that both knock-down conditions resulted in decreased H3K9me3 levels at *Dux* (Figure 3F), however, this was attributable to the lower levels of H3 itself (Figure 3G) as the ratio of the modified H3 to all H3 remained unchanged (Figure 3H). This result is suggestive of an increased chromatin accessibility at this locus and may explain the relatively subtle *Dux* expression changes upon knockdown of Lrif1 or Trim28.

Collectively, our findings identify a functional relationship between Lrif1 and Trim28 and support a conserved function of Lrif1 in the regulation of *Dux*/*DUX4* expression in mammals.

Material and Methods

Cell culture

E14 mouse embryonic stem cells (mESCs) were grown on 0.1% gelatin (Sigma, #G-1890) coated plates on an UV-irradiated feeder layer of MEFs. E14 mESCs were maintained in medium composed of KnockOut™ DMEM (Gibco, #10829018) supplemented with 10% FBS (Biowest, #S1810), 1x MEM Non-Essential Amino Acids Solution (Gibco, #11140050), 2 mM L-Glutamine (Gibco, #25030149), 1 mM Sodium Pyruvate (Gibco, #11360070), 0.1 mM 2-Mercaptoethanol (Gibco, #31350010) and 10^5 U/mL Leukemia Inhibitory Factor (EMD Millipore, #ESG1107). HEK293T cells were maintained in medium composed of Gibco DMEM, High Glucose, Pyruvate (Gibco, #119950) with addition of 10% FBS (Biowest, #S1810) and 1x Penicillin/streptomycin (Gibco, #15140122).

siRNA transfections

mESCs were reverse transfected with siGENOME siRNA SMARTpool (Horizon) at a final concentration of 40 nM using Lipofectamine™ RNAiMAX (Thermo Fisher Scientific, #13778030). siGENOME Non-Targeting Pool #2 was used as a negative control. Two days after the first transfection, cells were either harvested or 1/5th of the cells

were reverse transfected again as per the first transfection. Cells were harvested for subsequent analysis two days post-transfection.

RNA isolation
Cells were harvested in Qiazol (Qiagen, #79306) and total RNA was isolated using RNeasy mini kit (Qiagen, #74101) accompanied with on-column DNase I treatment.

cDNA synthesis followed by RT-qPCR
cDNA synthesis was performed with poly-dT primer using the RevertAid H Minus First Strand cDNA synthesis kit (Thermo Fisher Scientific, #K1621). Gene expression was analysed using iQ™ SYBR® Green Supermix (Biorad, #1708887) on a CFX384 Touch Real-Time PCR Detection System. All primers used for RT-qPCR are listed in Supplementary Table 3. mβ-actin was used as a housekeeping gene.

RNA processing for total RNA-seq
Total RNA was isolated as described above and RNA-seq was outsourced to Macrogen-Europe. Sequencing libraries were prepared with TruSeq Stranded Total RNA with Ribo-Zero Human/Mouse/Rat kit () according to the manufacturer's manual. Samples were sequenced as 100 bp paired-end on a HiSeq instrument.

RNA-seq data analysis
Quality assessment of the raw sequencing reads was done using FastQC v0.11.6. Adapters were removed by Trimmomatic v0.38 with parameters PE -threads 10 -phred33 ILLUMINACLIP:TruSeq3-PE.fa:2:30:10 LEADING:3 TRAILING:3 SLIDINGWINDOW:4:15 MINLEN:40. The remaining quality-filtered reads were aligned to the mouse reference genome mm10 with the corresponding annotation file from Ensemble using the STAR aligner v2.7.1 with parameters. A read count table was obtained with HTSeq-count v0.9.1 using the GENCODE MV23 annotation with the option "–stranded reverse". The differential expression statistical analysis was done with DESeq2 v1.24.0 (R package). In the design we included correction for known experimental and sequencing batch effects (see Suppl. Table 4). Otherwise, default settings were used except for siSmchd1 analysis, where differential expression analysis was done on pre-filtered data, where 78% of the lowest expressed genes (based on row-wise mean of normalized counts) was filtered out due to an otherwise faulty outcome when independent filtering was used. The final list of differential expressed genes contains genes for which the adjusted p-value (Benjamini-Hochberg correction) is <0.05. RNA-seq plots were generated with ggplot2 package v3.3.3.

Cloning
The open reading frames (ORFs) of Lrif1s and Lrif1l were subcloned first into pEF1a-FB-dCas9-puro (Addgene plasmid #100547) by replacing the Cas9 insert via NheI/XbaI sites. The Lrif1s/l ORFs were amplified using an N-terminal specific primer for either Lrif1s (mLrif1s NheI F: 5'-TCCTTGCTAGCATGGCATCAATAGTAAAAAAGGAAATTC-3') or Lrif1l (mLrif1l NheI F: 5'-TCCTTGCTAGCATGTCTAATAGTCTCCAGAGCG-3') combined with the same reverse primer (mLrif1 XbaI R: 5'-CCTCATCTAGATTATTGTTTTTGGTACATCTTCTTACGC-3'). Resulting plasmids were further modified by replacing the N-terminal FlagAvi tag with EGFP via BstbI/NheI sites. EGFP was amplified from the pEGFP-C1 plasmid using the following primers: EGFP BstbI F: 5'-GATCTTTCGAAAGCCACCATGGTGAGCAAGGG-3' & EGFP NheI R:5'-ACATGCTAGCAAGGATCCTCGAAGCTTGAGCTCGAGATC-3'). Control plasmid expressing only EGFP-NLS was created by replacing FlagAvi-Cas9 insert in pEF1a-FB-dCas9-puro with EGFP-NLS via BstbI/XbaI sites. EGFP-NLS was amplified from the C1-EGFP-NLS plasmid (king gift of Prof. Haico van Attikum; Leiden University Medical Center) with the following primers: EGFP BstbI F: 5'- GATCTTTCGAAAGCCACCATGGTGAGCAAGGG-3' & EGFP-NLS XbaI R: 5'-CCTCATCTAGACTAAACCTTTCTCTTCTTCTTAGGACC-3'). The two C-terminal Lrif1 mutants (denoted in the text as mPVL and m1) were introduced to both the short and the long Lrif1 isoform and were created by overlapping PCR with mutagenic primers carrying the respective mutations (for primers combinations see Supplementary Table S5). The respective pEF1a-EGFP-Lrif1s/l-puro plasmids were used as a template for creating inserts 1 and 2, which were subsequently used in the final merging PCR. The final PCR products were cloned in the pEF1a-EGFP-Lrif1s/l-puro via BamHI/XbaI, thus exchanging the Lrif1s/l WT ORFs with their mutant counterpart.

Western blotting
Samples were lysed with RIPA buffer (0.1% SDS, 1% Igepal CA-630, 150mM NaCl, 0.5% Sodium Deoxycholate, 20mM EDTA) supplemented with 1x Complete™, EDTA-free Protease Inhibitor Cocktail (PI) (Sigma-Aldrich, #11873580001). Samples were incubated on ice for 10 min followed by centrifugation at 15,000g for 15 min at

4°C. Protein concentration was determined with Pierce™ BCA Protein Assay Kit (Thermo Fisher Scientific, #23225). For western blotting, samples were first mixed with 6X sample buffer (0.375M Tris pH 6.8, 12% SDS, 60% glycerol, 0.6M DTT, 0.06% bromophenol blue) to 1x final concentration, boiled for 10 min at 95°C and resolved on Novex™ NuPAGE™ 4-12% Bis-Tris protein gels (Invitrogen, #NP0321BOX). Post-run gel was transferred to an Immobilon-FL PVDF membrane (Merck, #IPFL00010). The membrane was blocked for 1 h in 4% skim milk in PBS followed by incubation overnight at 4°C with primary antibodies diluted in Immuno Booster solution I (Takara, #T7111A): RαGFP (1:1000, Abcam, #ab290), RαSMCHD1 (1:1000, Abcam #ab31865), RαLRIF1 (1:1000, Proteintech, #26115-1-AP), MαKAP1 (1:1000, Abcam, #ab22553), MαHP1γ clone 42s2 (1:1000, EMD Millipore, #05-690) and Mα-αTubulin (1:4000, Sigma-Aldrich #T6199). The next day, membranes were washed twice with PBS-T (0.01% Tween-20) and incubated with the following secondary antibodies diluted in Immuno Booster solution II (Takara, #T7111A): IRDye® 800CW goat anti-rabbit IgG (1:10,000, Li-cor #P/N 925-32211) and IRDye® 680CW donkey anti-mouse IgG (1:10,000, #P/N 925-68072) for 1h at room temperature. Membranes were washed twice with PBS-T prior scanning on the Odyssey® CLx Imaging System (Li-cor).

Plasmids transfections

For co-immunoprecipitation with GFP-trap beads, $10x10^6$ mESCs were reverse transfected with 5 µg of plasmid DNA with Lipofectamine 3000 (Thermo Fisher Scientific, #L3000008) on a Ø6 cm dish with 0.1% gelatine. Each transfection condition was done in three biological replicates. 30h post-transfection, cells were harvested for downstream co-immunoprecipitation with GFP-trap beads. For GFP co-immunoprecipitation in HEK293T cells, $2.5x10^6$ cells were seeded one day prior plasmid transfection on a Ø10 cm dish. The next day, cells were transfected with 6 µg of plasmid DNA with polyethylenimine (PEI) in 1:3 volume ratio. Cells were harvested 30h post-transfection.

GFP-Trap co-immunoprecipitation for mass spectrometry

Transfected mESCs were washed 2x with ice-cold PBS and lysed on the dish with 600 µl of NP40 lysis buffer (50 mM Tris-HCl pH 8.0, 150 mM NaCl, 1% NP-40) supplemented with 1x PI, 20 mM NaF and 20 mM NEM. Whole cell lysates were incubated at 4°C, for 15 min while rotating, then spun down for 14,000g, 10 min at 4°C. 5% volume of supernatant was saved as input, mixed with 6xSB to a final 1X concentration and boiled for 10 min at 95°C. The remainder of the supernatant was added to 20 µl pre-washed GFP-Trap agarose beads (Chromotek, #gta-20) and incubated for 1.5 h at 4°C while rotating. Beads were subsequently washed 2x with NP40 lysis buffer followed by 3x wash with NP40 lysis buffer without NP40 and the final three washes were done with freshly prepared 50 mM ammonium bicarbonate (ABC). After the last wash, 10% of the beads was used for protein elution in 2xSB by boiling for 15 min at 95°C while shaking to check for IP efficiency by western blot. The rest of the beads were incubated overnight with 2.5 µg of sequencing grade trypsin (Promega, #V5111) (dissolved in 50 mM ABC) at 37°C while shaking. The next day, digested peptides were filtered through a pre-washed 0.45 µm filter (EMD Millipore, #UFC40LH25) followed by acidification through addition of trifluoroacetic acid (TFA) to a 2% final concentration. Peptide solutions were loaded on a custom-made Stage Tip as containing a disk made of tC18 cartridge (Waters, #WAT036820) as described previously [21]. Stage Tips were washed twice with 0.1% formic acid, and peptides were eluted with 2x 25 µl of 32.5% acetonitrile in 0.1 % formic acid. Eluates were vacuum dried with a SpeedVac RC10.10 and kept at -80°C.

Mass spectrometry data acquisition

Mass spectrometry data was acquired essentially as described in Gonzalez-Prieto et al. [22]. In brief, a Liquid Chromatography gradient was performed on an EASY-nLC 1000 system (Proxeon, Odense, Denmark) connected to a Q-Exactive Orbitrap (Thermo Fisher Scientific, Germany) through a nano-electrospray ion source. The Q-Exactive was coupled to a 20 cm analytical column with an inner-diameter of 75 µm, in-house packed with 1.9 µm C18-AQ beads (Reprospher-DE, Pur, Dr. Maish, Ammerbuch-Entringen, Germany). For each sample, two different acquisition methods were performed as technical repeats. The chromatography gradient length was 70 minutes from 2% to 30% acetonitrile in followed by 5 minutes gradient to 95% acetonitrile in 0.1% formic acid prior to column re-equilibration at a flow rate of 200 nL/minute. The mass spectrometer was operated in data-dependent acquisition (DDA) mode. The first technical repeat was performed with a top-10 method. The maximum MS1 and MS2 injection times were 250 ms and 60 ms, respectively. For the second technical repeat, a Top5 method was used with MS1 and MS2 injection times being 250 ms and 256 ms, respectively. In both technical repeats, full-scan MS spectra were acquired in a range from 300 to 1600 m/z at a target value of 3×10^6 and a resolution of 70,000 and the Higher-Collisional Dissociation (HCD) tandem mass spectra (MS/MS) were recorded at a target value of 1×10^5 with a resolution of 17,500. Minimum AGC target was set to 1×10^4 and the normalized collision energy (NCE) was set to 25. The isolation window was 2.2

m/z wide. The precursor ion masses of scanned ions were dynamically excluded (DE) from MS/MS analysis for 20 sec. Ions with charge 1, and greater than 6 were excluded from triggering MS2 analysis.

Mass spectrometry data analysis

LC-MS/MS Raw files were analyzed using MaxQuant software (v1.6.14) according to Tyanova et al.[23] using default settings with the following modifications. Maximum number of mis-cleavages by trypsin/p was set to 3. Variable modifications included Oxidation (M), Acetyl (Protein N-terminus) and Phospho (STY) with a maximum number per peptide of 3. Carbamidomethyl (C) was deactivated as fixed modification. Label-free Quantification was enabled without the Fast LFQ algorithm. We performed the search against an in silico digested UniProt reference proteome for Homo sapiens (19th Sep 2019). The match-between-runs feature was enabled with a 0.7 min match time window and 20 min alignment time window. Protein quantification included all the peptides. MaxQuant proteingroups.txt file output was further analyzed using the Perseus computational platform (v1.6.14) as described by Tyanova et al.[23]. Potential contaminants and reverse peptides were removed, the matrix was log2 transformed and proteins not identified in 3 out of 3 replicates for at least one condition were also removed. Missing values were randomly imputed from normal distribution width of 0.3 and a downshift of 1.8. Statistical conditions between the groups were calculated by t-test with a permutation based FDR of 0.05 and an S0 of 0.1. Statistical tables were exported and data was further processed in Microsoft Excel 365 for comprehensive visualization.

GFP-Trap co-immunoprecipitation with Lrif1 mutants in HEK293T cells

Transfected HEK293T cells were washed 2x with ice-cold PBS and lysed on the dish with 1 ml of NP40 lysis buffer (50 mM Tris-HCl pH 8.0, 150 mM NaCl, 1% NP-40) supplemented with 1x PI, 20 mM NaF, 20 mM NEM, 2 mM $MgCl_2$ and 250U Benzonase (EMD Millipore, #E1014). Whole cell lysates were incubated at 4°C, for 1 h while rotating, then spun down for 14,000g, 10 min at 4°C. 1 mg of whole cell lysate was added to 20 µl pre-washed GFP-Trap agarose beads and incubated for 1.5 h at 4°C while rotating. Beads were washed 4x with NP40 lysis buffer and proteins were eluted by boiling the beads in 2xSB at 95°C for 15 min while shaking. Input samples represent 2% of material used for IP.

Endogenous co-immunoprecipitation in mESCs

mESCs were washed 2x with ice-cold PBS and lysed on the dish with EBC lysis buffers (50 mM Tris-HCl pH 8.0, 150 mM NaCl, 0.5% NP-40, 2 mM $MgCl_2$) supplemented with 1x PI, 20 mM NaF and 20 mM NEM. Whole cell lysates were incubated at 4°C, for 15 min while rotating, then spun down for 14,000g, 10 min at 4°C. 500 µg of the whole cell lysate was added to 20 µl of antibody pre-linked Dynabeads and incubated overnight at 4°C while rotating. Protein A Dynabeads (Thermo Fisher Scientific, #10002D) were used for conjugation of the antibodies of rabbit origin and protein G Dynabeads (Thermo Fisher Scientific,#10003D) were used for Co-IP with the antibodies of mouse origin. The following antibodies were used for endogenous Co-IPs: RαKap1 (Abcam, #ab10483), RαLRIF1 (Proteintech, #26115-1-AP), RαIgG (Cell Signalling, #2729S), MαKap1 (Abcam, #ab22553) and MαIgG (Merck, #12-371). The next day, beads were washed 4x with EBC lysis buffer and proteins were eluted by boiling the beads in 2xSB at 95°C for 15 min while shaking.

Chromatin immunoprecipitation followed by qPCR

Feeder MEFs were removed by pre-plating the trypsinized cell suspension 2x for 20 min on gelatinized culture plates. The supernatant was collected and washed once in 1x warm PBS followed by crosslinking with 1% formaldehyde in PBS for 10 min at room temperature while tumbling. The reaction was quenched by adding glycine to a final concentration of 125 mM. Crosslinked cells were washed twice with PBS and the cell pellet was either stored at -80°C or proceeded to chromatin isolation. Cell pellets were resuspended in ice-cold ChIP buffer (1.5 ml lysis buffer/10 x 10^6 cells) (150 mM NaCl, 50 mM Tris-HCl pH 7.5, 5 mM EDTA, 0.5 % Igepal CA-630, 1% Triton X-100) supplemented with Complete' Protease Inhibitor Cocktail tablet (Sigma-Aldrich, #11697498001). After 10 min incubation on ice, samples were spun down at 8,000 g for 2 min at 4°C. The pellets were resuspended for the second time in ChIP buffer, incubated for 5 min on ice and spun down again. The final nuclear pellets were resuspended in ChIP buffer and sonicated at the highest power output for 15 cycles (1 cycle: 30 sec ON/30 sec OFF) using a Bioruptor instrument (Diagenode). For ChIP, chromatin was first pre-cleared with BSA-blocked protein A Sepharose beads (GE Healthcare, #17-5280-21) by rotating for 30-60 min at 4°C. For histone ChIP, 6 µg of chromatin was used and for Trim28 ChIP, 30 µg of chromatin was used in a final volume of 500 µl. 50 µl (10%) of each chromatin was kept as input sample for later normalization. ChIP was carried out by rotation at 4°C with following primary antibodies: RαTrim28 (Abcam, #ab10483), RαH3 (Abcam, ab1791), RαH3K9me3 (Active Motif,

#39161) or rabbit polyclonal IgG (Abcam, #ab37415), which served as a negative control. The second day, 20 µl of protein A Sepharose beads pre-blocked with BSA were added to all samples and incubated for 2 h at 4°C while rotating. Afterwards, beads were washed as follows: once with low salt wash buffer (1 % Triton X-100, 0.1 % SDS, 2 mM EDTA, 20 mM Tris-HCl, 150 mM NaCl), high salt wash buffer (1 % Triton X-100, 0.1 % SDS, 2 mM EDTA, 20 mM Tris-HCl, 500 mM NaCl), LiCl wash buffer (250 mM LiCl, 1% Igepal CA-630, 1% sodium deoxycholate, 1 mM EDTA, 10 mM Tris-HCl) and twice with TE wash buffer (10 mM Tris-HCl, 1 mM EDTA). For DNA extraction, 10% (w/v) of Chelex 100 resin was added to the beads and boiled at 95°C for 15 min while vigorously shaking. Supernatant was used for qPCR analysis at 60°C using following primers for the *Dux* locus: Dux ChIP F2 5'-CTAGCGACTTGCCCTCCTTCTG-3' and Dux ChIP R2: 5'-ATTCAGAGGGGCTGGAGCAG-3'; *en masse* IAPEz[10]: IAPEz fwd 5'- ACGGGAACACTTCATTACCACC-3' and IAPEz rev 5'- TTGAGAAGGATTCAACTGCGTG-3'; Gapdh int2[24]: Gapdh_int2 F 5'- ATCCTGTAGGCCAGGTGATG-3' and Gapdh_int2 R 5'- AGGCTCAAGGGCTTTTAAGG-3'.

Acknowledgements

We would like to thank members of van der Maarel group for critical reading of the manuscript. DS, JB and SMVDM are members of the European Reference Network for Rare Neuromuscular Diseases [ERN EURO-NMD] and/or members of the Netherlands Neuromuscular Center (NL-NMD). This work was supported by funds from the National Institute of Arthritis and Musculoskeletal and Skin Diseases (NIAMS) grant number R01AR045203 and the Prinses Beatrix Spierfonds grant number W.OR15-26.

Conflict of interest

Authors declare no conflict of interest.

References

1. Akiyama, T. *et al.* Transient bursts of Zscan4 expression are accompanied by the rapid derepression of heterochromatin in mouse embryonic stem cells. *DNA Res.* **22**, 307–318 (2015).
2. Eckersley-Maslin, M. A. A. *et al.* MERVL/Zscan4 Network Activation Results in Transient Genome-wide DNA Demethylation of mESCs. *Cell Rep.* **17**, 179–192 (2016).
3. Macfarlan, T. S. *et al.* Embryonic stem cell potency fluctuates with endogenous retrovirus activity. *Nature* **487**, 57–63 (2012).
4. Zhang, W. *et al.* Zscan4c activates endogenous retrovirus MERVL and cleavage embryo genes. *Nucleic Acids Res.* **47**, 8485–8501 (2019).
5. Genet, M. & Torres-Padilla, M.-E. The molecular and cellular features of 2-cell-like cells: a reference guide. *Development* **147**, (2020).
6. Hendrickson, P. G. *et al.* Conserved roles of mouse DUX and human DUX4 in activating cleavage-stage genes and MERVL/HERVL retrotransposons. *Nat. Genet.* **49**, 925–934 (2017).
7. Percharde, M. *et al.* A LINE1-Nucleolin Partnership Regulates Early Development and ESC Identity. *Cell* **174**, 391-405.e19 (2018).
8. Huang, Z. *et al.* The chromosomal protein SMCHD1 regulates DNA methylation and the 2c-like state of embryonic stem cells by antagonizing TET proteins. *Sci. Adv.* **7**, eabb9149 (2021).
9. Cossec, J. C. *et al.* SUMO Safeguards Somatic and Pluripotent Cell Identities by Enforcing Distinct Chromatin States. *Cell Stem Cell* **23**, 742-757.e8 (2018).
10. De Iaco, A. *et al.* DUX-family transcription factors regulate zygotic genome activation in placental mammals. *Nat. Genet.* **49**, 941–945 (2017).
11. Eckersley-Maslin, M. *et al.* Dppa2 and Dppa4 directly regulate the Dux-driven zygotic transcriptional program. *Genes Dev.* **33**, 194–208 (2019).
12. Li, H. J., Haque, Z. K., Chen, A. & Mendelsohn, M. RIF-1, a novel nuclear receptor corepressor that associates with the nuclear matrix. *J. Cell. Biochem.* **102**, 1021–1035 (2007).
13. Akram, S. *et al.* LRIF1 interacts with HP1α to coordinate accurate chromosome segregation during mitosis. *J. Mol. Cell Biol.* (2018) doi:10.1093/jmcb/mjy040.
14. Brideau, N. J. *et al.* Independent Mechanisms Target SMCHD1 to Trimethylated Histone H3 Lysine 9-Modified Chromatin and the Inactive X Chromosome. *Mol. Cell. Biol.* **35**, 4053–68 (2015).
15. Nozawa, R.-S. *et al.* Human inactive X chromosome is compacted through a PRC2-independent SMCHD1-HBiX1 pathway. *Nat. Struct. Mol. Biol.* **20**, 566–573 (2013).
16. Stoll, G. A. *et al.* Structure of KAP1 tripartite motif identifies molecular interfaces required for retroelement silencing. *Proc. Natl. Acad. Sci. U. S. A.* **116**, 15042–15051 (2019).
17. Lomberk, G., Wallrath, L. & Urrutia, R. The Heterochromatin Protein 1 family. *Genome Biol.* **7**, 228 (2006).
18. Maksakova, I. A. *et al.* Distinct roles of KAP1, HP1 and G9a/GLP in silencing of the two-cell-specific retrotransposon MERVL in mouse ES cells. *Epigenetics and Chromatin* **6**, 15 (2013).
19. Rowe, H. M. *et al.* KAP1 controls endogenous retroviruses in embryonic stem cells. *Nature* **463**, 237–240 (2010).
20. Rowe, H. M. *et al.* TRIM28 repression of retrotransposon-based enhancers is necessary to preserve transcriptional dynamics in embryonic stem cells. *Genome Res.* **23**, 452–461 (2013).
21. Rappsilber, J., Mann, M. & Ishihama, Y. Protocol for micro-purification, enrichment, pre-fractionation and storage of peptides for proteomics using StageTips. *Nat. Protoc.* **2**, 1896–1906 (2007).
22. González-Prieto, R. *et al.* Global non-covalent SUMO interaction networks reveal SUMO-dependent stabilization of the non-homologous end joining complex. *Cell Rep.* **34**, 108691 (2021).
23. Tyanova, S., Temu, T. & Cox, J. The MaxQuant computational platform for mass spectrometry-based shotgun proteomics. *Nat. Protoc.* **11**, 2301–2319 (2016).
24. Matsui, T. *et al.* Proviral silencing in embryonic stem cells requires the histone methyltransferase ESET. *Nat. 2010 4647290* **464**, 927–931 (2010).

Supplementary Information

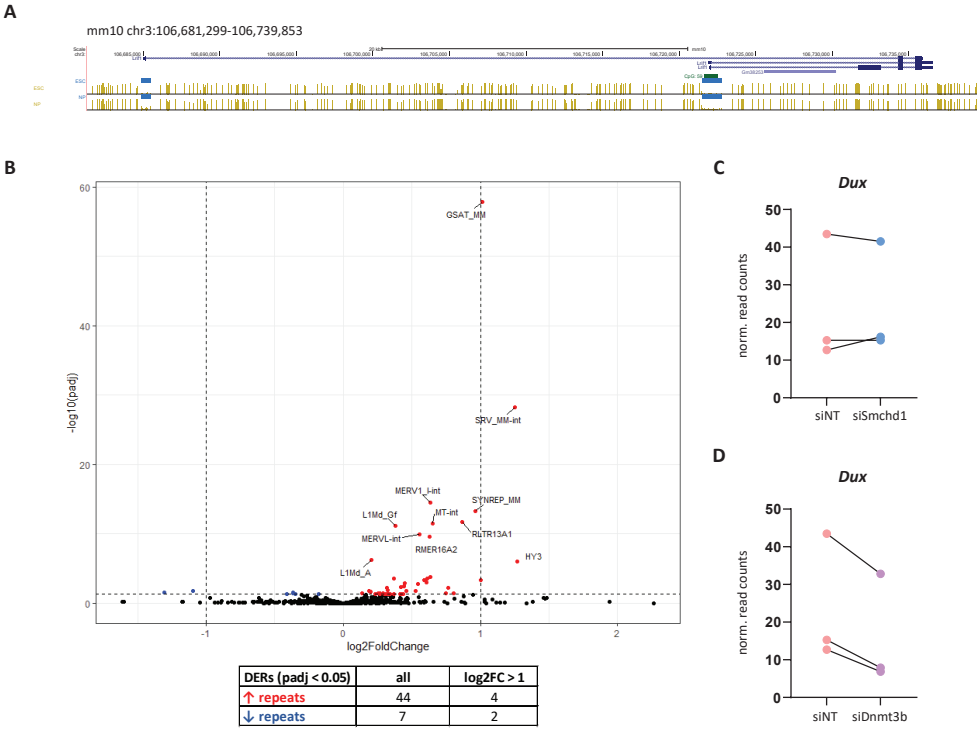

DERs (padj < 0.05)	all	log2FC > 1
↑ repeats	44	4
↓ repeats	7	2

Suppl. Figure 1. Lrif1 knock-down causes upregulation of 2C-specific repeats. A) Snapshot of *Lrif1* locus from UCSC genome browser (mm10) showing three *Lrif1* isoforms. Whole-genome bisulfite sequencing tracks showing mouse embryonic stem cell (ESC) and neuronal (NP) methylomes over *Lrif1* locus from Stadler et al.[25] (available from DNA methylation hub for mm10 in UCSC genome browser) . Regional hypomethylation over two different *Lrif1* transcriptional start sites is marked with blue boxes. **B)** Volcano plot showing expression changes of repeats following Lrif1 knock-down. Upregulated repeats are highlighted in red and downregulated repeats are highlighted in blue. Dashed lines indicate a fold change of two (log_2 fold of 1) on the x axis and significance of 0.05 (–log10 p.adj of 1.3) on the y axis. The top 10 differentially expressed repeats (DERs) are labelled. Table summary of DERs is provided below the plot. **C)** Normalized read counts of *Dux* transcripts after Smchd1 knock- down compared to non-targeting siRNA condition. **D)** Normalized read counts of *Dux* transcripts after Dnmt3b knock down compared to non-targeting siRNA condition.

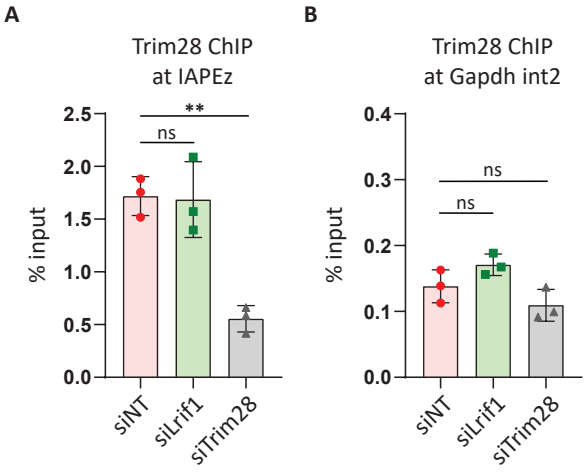

Suppl. Figure 2. Lrif1 does not affect Trim28 binding to IAPEz. Trim28 ChIP-qPCR of **A)** IAPEz elements, **B)** intron 2 of *Gapdh* in E14 mESCs after treatment with respective siRNAs. Bars and whiskers represent mean ± SEM of three independent experiments. Statistical significance was calculate by one-way ANOVA with Dunnett's post hoc test (ns: not significant; *: < 0.05, **: < 0.01).

Suppl. Table 1. Commonly identified differentially up- and downregulated genes in all three knock-down conditions related to Figure 1 G & H.

Common differentially upregulated genes

ensembl_gene_id	mgi_symbol	chr	start	end	strand
ENSMUSG00000039202	Abhd2	7	78922947	79015256	1
ENSMUSG00000069833	Ahnak	19	8966648	9054278	1
ENSMUSG00000032826	Ank2	3	126715261	127292999	-1
ENSMUSG00000029338	Antxr2	5	98030642	98178902	-1
ENSMUSG00000031511	Arhgef7	8	11777721	11885219	1
ENSMUSG00000024501	Dpysl3	18	43454049	43571351	-1
ENSMUSG00000026131	Dst	1	33947306	34347742	1
ENSMUSG00000003518	Dusp3	11	101861969	101877839	-1
ENSMUSG00000025278	Flnb	14	14518185	14651816	-1
ENSMUSG00000022816	Fstl1	16	37597235	37656876	1
ENSMUSG00000025241	Fyco1	9	123618565	123680964	-1
ENSMUSG00000020176	Grb10	11	11880508	11988683	-1
ENSMUSG00000027007	Itprid2	2	79465696	79503310	1
ENSMUSG00000026478	Lamc1	1	153094668	153208532	-1
ENSMUSG00000031207	Msn	X	95139648	95212158	1
ENSMUSG00000024177	Nme4	17	26310708	26314576	-1
ENSMUSG00000063972	Nr6a1	2	38613382	38817700	-1
ENSMUSG00000039191	Rbpj	5	53623494	53814704	1
ENSMUSG00000037071	Scd1	19	44382894	44396318	-1
ENSMUSG00000025203	Scd2	19	44282113	44295303	1
ENSMUSG00000061186	Sfmbt2	2	10375321	10600064	1
ENSMUSG00000020422	Tns3	11	8381652	8614681	-1
ENSMUSG00000051747	Ttn	2	76534324	76812891	-1

Common differentially downregulated genes

ensembl_gene_id	mgi_symbol	chr	start	end	strand
ENSMUSG00000003309	Ap1m2	9	21205571	21223633	-1
ENSMUSG00000028218	Cibar1	4	12153409	12172015	-1
ENSMUSG00000027552	E2f5	3	14643701	14671369	1
ENSMUSG00000015937	Macroh2a1	13	56221432	56284174	-1
ENSMUSG00000004891	Nes	3	87878385	87887758	1
ENSMUSG00000040204	Pclaf	9	65797519	65810548	1
ENSMUSG00000028134	Ptbp2	3	119512391	119578115	-1
ENSMUSG00000032487	Ptgs2	1	149975782	149983978	1
ENSMUSG00000028464	Tpm2	4	43514711	43523765	-1

Suppl. Table 2. Statistical analysis of the proteins identified by mass spectrometry in the different GFP-tagged Lrif1 isoforms co-immunoprecipitation assays related to Figure 2 A & B.

GENE		Lrif1 short vs Control				Lrif1 long vs Control			
Uniprot ID	Gene names	Significant (FDR=0.05 S0=0.1)	-Log p-value	q-value	Difference (log2)	Significant (FDR=0.05 S0=0.1)	-Log p-value	q-value	Difference (log2)
Q6P5D8	Smchd1	+	3,62	0,00	11,80	+	3,40	0,00	10,32
P83917	Cbx1	+	4,25	0,00	11,38	+	3,49	0,00	7,36
Q8CDD9	Lrif1	+	2,77	0,00	10,55	+	2,50	0,00	8,93
Q61686	Cbx5	+	6,00	0,00	9,63	+	5,03	0,00	5,39
Q9DCC5	Cbx3	+	2,19	0,00	8,75	+	1,66	0,00	5,59
Q01320	Top2a	+	1,59	0,00	5,47		0,21	0,59	-0,91
Q91W39	Ncoa5	+	4,14	0,00	4,63		NaN	1,00	0,00
Q921K2	Parp1	+	3,47	0,00	3,92	+	1,02	0,01	-2,28
P62806	Hist1h4a	+	2,16	0,00	2,67	+	1,55	0,00	-2,29
Q60749	Khdrbs1	+	3,81	0,00	2,62	+	1,15	0,01	-0,66
E0CZ27	H3f3a	+	1,50	0,00	2,61		0,51	0,14	-1,16
Q8CBB6	Hist1h2br	+	2,03	0,00	2,56	+	1,35	0,01	-1,91
Q8CGP5	Hist1h2af	+	1,79	0,00	2,51	+	1,31	0,01	-2,12
A0A0R4J0I9	Lrp1	+	2,56	0,00	1,98		NaN	1,00	0,00
A2ARV4	Lrp2	+	1,97	0,00	1,95		0,54	0,14	0,63
Q61696	Hspa1a	+	2,31	0,00	1,95		0,81	0,05	0,62
P62334	Psmc6	+	2,50	0,00	1,94		0,36	0,31	0,70
A0A2I3BRL8	Rbmxl1	+	3,18	0,00	1,74	+	2,26	0,00	-0,56
Q91VI7	Rnh1	+	2,54	0,00	1,74	+	3,67	0,00	3,28
P17427	Ap2a2	+	1,78	0,00	1,62	+	1,85	0,00	1,68
Q923G2	Polr2h	+	2,22	0,00	1,52	+	2,53	0,00	1,88
Q8R0G9	Nup133	+	0,93	0,03	1,51	+	1,90	0,00	3,39
Q9ERD7	Tubb3	+	2,04	0,00	1,48	+	3,76	0,00	2,56
Q8BH74	Nup107	+	1,13	0,02	1,46	+	2,31	0,00	3,25
Q9DAE2	Rbmxl2	+	0,86	0,03	1,44		0,52	0,14	0,83
P63166	Sumo1	+	0,86	0,04	1,31	+	1,86	0,00	1,14
Q9WV32	Arpc1b	+	1,76	0,00	1,30		NaN	1,00	0,00
Q9D883	U2af1		0,64	0,09	1,26	+	0,75	0,04	1,45
P14115	Rpl27a	+	3,75	0,00	1,20	+	3,37	0,00	0,74
Q6ZWZ4	Rpl36	+	3,12	0,00	1,14	+	3,22	0,00	1,04
Q99KP6	Prpf19	+	1,70	0,00	1,13		0,19	0,71	0,24
Q60848-2	Hells	+	1,55	0,01	1,10	+	1,28	0,01	0,76
P62242	Rps8	+	6,03	0,00	1,09	+	4,95	0,00	1,04
P47963	Rpl13	+	2,76	0,00	1,03	+	4,08	0,00	1,12
P61514	Rpl37a	+	1,11	0,02	1,00	+	1,05	0,01	0,93
Q9R0Q7	Ptges3	+	2,19	0,00	0,99	+	3,08	0,00	1,90
P63017	Hspa8	+	3,27	0,00	0,99	+	4,03	0,00	1,53
Q9CR57	Rpl14	+	2,46	0,00	0,98	+	3,12	0,00	1,14
A0A0G2JDW7	Rps27	+	3,59	0,00	0,97	+	2,83	0,00	0,75
Q8BP67	Rpl24	+	3,05	0,00	0,96	+	3,53	0,00	1,10
F8WHL2	Copa		0,80	0,06	0,96	+	0,79	0,04	0,90
P25444	Rps2	+	2,22	0,00	0,93	+	2,67	0,00	0,97

GENE		Lrif1 short vs Control				Lrif1 long vs Control			
Uniprot ID	Gene names	Significant (FDR=0.05 S0=0.1)	-Log p-value	q-value	Difference (log2)	Significant (FDR=0.05 S0=0.1)	-Log p-value	q-value	Difference (log2)
Q9CZM2	Rpl15	+	2,75	0,00	0,92	+	3,10	0,00	0,96
P14148	Rpl7	+	3,25	0,00	0,89	+	2,93	0,00	1,15
O55142	Rpl35a	+	3,09	0,00	0,88	+	2,62	0,00	1,39
P27659	Rpl3	+	2,42	0,00	0,88	+	2,64	0,00	0,93
P20029	Hspa5	+	4,27	0,00	0,88	+	3,15	0,00	0,54
P62702	Rps4x	+	2,50	0,00	0,87	+	2,63	0,00	0,97
P62849-2	Rps24	+	3,45	0,00	0,87	+	2,85	0,00	0,94
A0A1D5RLW5	Rpl18a	+	3,01	0,00	0,87	+	3,59	0,00	1,08
P12970	Rpl7a	+	3,09	0,00	0,87	+	4,39	0,00	1,28
P19253	Rpl13a	+	3,35	0,00	0,84	+	4,06	0,00	1,26
P62855	Rps26	+	2,80	0,00	0,83	+	2,38	0,00	1,19
P68369	Tuba1a		0,34	0,38	0,83	+	0,81	0,03	1,72
P15864	Hist1h1c	+	1,04	0,03	0,82		0,44	0,36	0,24
P62889	Rpl30	+	1,07	0,03	0,81	+	2,19	0,00	0,99
Q9D8E6	Rpl4	+	6,61	0,00	0,80	+	3,74	0,00	1,20
Q99MN1	Kars	+	1,18	0,02	0,80	+	3,07	0,00	2,86
P62751	Rpl23a	+	3,79	0,00	0,79	+	3,96	0,00	1,21
A0A3B2WDD2	Rpl10a	+	2,74	0,00	0,78	+	3,91	0,00	0,90
P99027	Rplp2	+	3,17	0,00	0,78	+	3,10	0,00	0,91
I7HLV2	Rpl10	+	2,55	0,00	0,76	+	3,15	0,00	0,83
Q9JKX6	Nudt5		0,73	0,08	0,76	+	2,23	0,00	1,97
Q62318	Trim28	+	2,51	0,00	0,76	+	3,39	0,00	0,97
Q9CQM8	Rpl21	+	2,75	0,00	0,76	+	3,17	0,00	0,89
P14869	Rplp0	+	2,50	0,00	0,74	+	2,66	0,00	1,07
Q3U4X8	Lig1		0,44	0,25	0,71	+	1,15	0,01	1,41
Q99ME9	Gtpbp4		0,59	0,15	0,71	+	1,89	0,00	0,73
P47911	Rpl6	+	2,78	0,00	0,69	+	3,58	0,00	1,10
Q99L45	Eif2s2	+	2,57	0,00	0,69	+	3,46	0,00	1,27
D3Z2H7	Ctnnd1		0,27	0,51	0,69	+	2,58	0,00	3,19
D6RH49	Rps27l		0,36	0,36	0,69	+	1,98	0,00	1,90
P61358	Rpl27	+	2,38	0,00	0,68	+	3,77	0,00	0,88
P61255	Rpl26	+	1,53	0,01	0,68	+	2,22	0,00	1,14
P35980	Rpl18	+	1,76	0,01	0,67	+	2,35	0,00	0,88
D3YTQ9	Rps15	+	1,61	0,01	0,66	+	2,12	0,00	0,87
P62267	Rps23	+	1,74	0,01	0,65	+	2,43	0,00	1,01
P62918	Rpl8	+	2,94	0,00	0,65	+	3,88	0,00	1,26
P62900	Rpl31	+	3,67	0,00	0,65	+	1,59	0,00	1,57
P35979	Rpl12	+	2,43	0,00	0,64	+	3,12	0,00	0,90
A0A1B0GRR3	Rps11	+	1,20	0,03	0,63	+	3,58	0,00	0,78
P41105	Rpl28	+	1,99	0,01	0,62	+	2,70	0,00	1,17
P49718	Mcm5	+	3,77	0,00	0,62	+	3,85	0,00	0,86
P62192	Psmc1		0,68	0,11	0,61	+	1,42	0,01	1,21
Q8BVQ9	Psmc2		0,94	0,06	0,59	+	2,95	0,00	1,35
H3BKN0	Nsun2	+	2,44	0,00	0,59	+	3,68	0,00	1,15

GENE		Lrif1 short vs Control				Lrif1 long vs Control			
Uniprot ID	Gene names	Significant (FDR=0.05 S0=0.1)	-Log p-value	q-value	Difference (log2)	Significant (FDR=0.05 S0=0.1)	-Log p-value	q-value	Difference (log2)
Q6ZWX6	Eif2s1	+	3,05	0,00	0,58	+	4,39	0,00	1,12
P63087	Ppp1cc		0,33	0,43	0,57	+	0,83	0,03	1,27
Q6ZWN5	Rps9	+	2,32	0,00	0,57	+	3,41	0,00	1,09
Q9D1R9	Rpl34	+	1,24	0,03	0,57	+	2,11	0,00	0,95
P62301	Rps13	+	1,75	0,01	0,56	+	4,04	0,00	1,01
Q8VEK3-2	Hnrnpu	+	1,66	0,01	0,54	+	1,94	0,00	0,68
Q8C2Q3	Rbm14		0,33	0,44	0,52	+	1,24	0,01	1,29
P97351	Rps3a	+	2,07	0,01	0,51	+	2,73	0,00	0,82
Q6ZWZ7	Rpl17	+	1,70	0,01	0,50	+	2,20	0,00	0,88
Q5M8M8	Rpl29		0,65	0,14	0,50	+	1,23	0,01	0,86
A0A1L1SQA8	Rps25	+	1,88	0,01	0,50	+	2,34	0,01	0,43
Q7TPV4	Mybbp1a	+	2,95	0,00	0,50	+	2,75	0,00	0,54
Q99LE6	Abcf2	+	1,60	0,02	0,48	+	2,46	0,00	0,95
A2A547	Rpl19	+	1,41	0,02	0,47	+	2,66	0,00	1,03
Q9Z2X1	Hnrnpf	+	2,36	0,01	0,47	+	4,41	0,00	1,36
Q8BJY1	Psmd5	+	1,27	0,03	0,46	+	3,23	0,00	1,51
Q6ZWV7	Rpl35	+	1,86	0,01	0,46	+	2,34	0,00	1,25
A0A494BAX5	Nars	+	2,21	0,01	0,45	+	2,79	0,00	1,18
P62754	Rps6	+	1,98	0,01	0,43	+	2,96	0,00	0,72
P62264	Rps14	+	1,20	0,04	0,43	+	3,18	0,00	0,69
P83882	Rpl36a		0,99	0,06	0,42	+	1,53	0,01	0,85
F6YVP7	Gm10260	+	1,32	0,03	0,41	+	3,25	0,00	0,70
A0A0A6YW67	Gm8797		0,47	0,30	0,39	+	2,26	0,00	-1,50
A0A0H2UH27	Fxr1		0,90	0,09	0,39	+	1,58	0,01	0,73
P62245	Rps15a	+	2,02	0,02	0,39		0,54	0,40	0,15
Q61881	Mcm7	+	2,05	0,02	0,38	+	3,02	0,00	0,74
Q62167	Ddx3x	+	1,28	0,05	0,37	+	2,27	0,00	0,60
A0A087WPL5	Dhx9	+	1,56	0,03	0,37		1,18	0,06	0,26
P62960	Ybx1		0,41	0,36	0,37	+	1,15	0,01	1,09
O88477	Igf2bp1	+	1,57	0,03	0,35	+	2,63	0,00	0,67
P54276	Msh6	+	1,60	0,03	0,35	+	2,12	0,01	0,54
P55302	Lrpap1		0,60	0,22	0,34	+	1,61	0,01	-0,64
Q8BTS0	Ddx5	+	1,55	0,03	0,33	+	2,75	0,00	0,55
P05213	Tuba1b	+	2,38	0,02	0,32	+	4,29	0,00	1,33
P62911	Rpl32		1,28	0,06	0,30	+	2,42	0,00	1,18
Q9CZX8	Rps19		0,53	0,31	0,27	+	2,44	0,00	1,02
P68372	Tubb4b		1,00	0,12	0,27	+	3,30	0,00	0,85
Q60668-3	Hnrnpd		0,98	0,12	0,27	+	1,45	0,01	0,43
Q3UKJ7	Smu1		0,31	0,53	0,27	+	1,22	0,03	0,38
P61979-2	Hnrnpk	+	2,72	0,02	0,26	+	3,92	0,00	0,50
Q3U741	Ddx17		0,74	0,21	0,25	+	1,41	0,01	0,48
P17918	Pcna		0,61	0,28	0,24	+	2,35	0,00	0,85
Q9JJI8	Rpl38		1,03	0,14	0,23	+	2,27	0,00	0,72
P16460	Ass1		1,10	0,13	0,22	+	3,09	0,00	0,55

GENE		Lrif1 short vs Control				Lrif1 long vs Control			
Uniprot ID	Gene names	Significant (FDR=0.05 S0=0.1)	-Log p-value	q-value	Difference (log2)	Significant (FDR=0.05 S0=0.1)	-Log p-value	q-value	Difference (log2)
Q3KQM4	U2af2		0,76	0,23	0,22	+	1,93	0,01	0,41
P14131	Rps16		0,39	0,51	0,19	+	1,34	0,01	0,50
A0A140LIZ5	Psmc4		0,46	0,45	0,18	+	2,29	0,00	0,81
Q61553	Fscn1		1,21	0,20	0,16	+	2,17	0,01	0,35
A2AGN7	Psmc3		0,57	0,42	0,16	+	1,42	0,01	0,44
Q9CWF2	Tubb2b		0,49	0,48	0,15	+	3,05	0,00	1,11
P51881	Slc25a5		1,16	0,26	0,14	+	1,97	0,01	0,43
Q8K1K2	Psmc5		0,96	0,40	0,11	+	3,77	0,00	0,60
P09405	Ncl		0,53	0,55	0,11	+	0,98	0,03	0,58
P52480	Pkm		0,55	0,55	0,11	+	2,05	0,01	0,41
Q8C0C7	Farsa		0,36	0,67	0,09	+	2,49	0,00	0,64
Q9R0N0	Galk1		0,42	0,67	0,08	+	2,99	0,00	0,76
P27612	Plaa		0,52	0,66	0,07	+	4,99	0,00	1,65
P35486	Pdha1		0,13	0,84	0,06	+	1,15	0,03	0,41
P29595	Nedd8		0,08	0,89	0,05	+	1,68	0,01	-0,53
Q91YZ2	Ctbp2		0,14	0,85	0,05	+	2,38	0,00	0,69
G5E902	Slc25a3		0,20	0,84	0,04	+	2,01	0,01	0,40
Q9R1T2-2	Sae1		0,04	0,95	0,02	+	1,60	0,01	0,61
P80315	Cct4		0,05	0,97	0,01	+	1,85	0,01	0,35
P99024	Tubb5		0,03	0,98	0,00	+	2,80	0,00	0,76
Q45VK5	Ilf3		NaN	1,00	0,00	+	1,36	0,01	1,00
D3Z7K0	Otub1		NaN	1,00	0,00	+	1,31	0,01	0,53
P70404	Idh3g		NaN	1,00	0,00	+	1,57	0,00	1,62
Q9CQM5	Txndc17		NaN	1,00	0,00	+	1,71	0,00	2,26
A0A087WPE4	Tceb1		0,02	0,97	-0,02	+	1,13	0,01	0,70
P60843	Eif4a1		0,23	0,87	-0,03	+	2,47	0,01	0,30
P51410	Rpl9		0,21	0,84	-0,04	+	2,05	0,01	-0,50
P09103	P4hb		0,17	0,84	-0,04	+	1,15	0,01	-0,61
P20152	Vim		0,02	0,97	-0,05	+	1,18	0,01	-1,53
E9Q242	Adsl		0,22	0,79	-0,06	+	2,36	0,00	0,49
E9QAI5	Cad		0,81	0,63	-0,07	+	4,34	0,00	0,79
E9QN08	Eef1d		0,25	0,73	-0,09	+	1,86	0,01	0,52
Q922D8	Mthfd1		0,23	0,73	-0,10	+	1,11	0,03	-0,43
P80317	Cct6a		0,50	0,56	-0,11	+	1,97	0,01	0,38
P80318	Cct3		0,52	0,54	-0,12	+	1,81	0,01	0,40
Q01853	Vcp		0,85	0,37	-0,13	+	2,95	0,00	-1,01
P62137	Ppp1ca		0,34	0,58	-0,16	+	4,36	0,00	0,71
D3YZX3	Gnb2		0,11	0,82	-0,16	+	1,67	0,00	1,01
P25206	Mcm3		0,42	0,51	-0,16	+	1,42	0,03	0,33
A2AM74	Kif17		1,58	0,12	-0,18	+	0,84	0,04	-0,77
P68134	Acta1		0,15	0,77	-0,19	+	1,48	0,00	-2,21
Q9EST5	Anp32b		0,09	0,84	-0,19	+	0,87	0,02	1,67
A0A2R8W6Y5	Larp4		0,78	0,24	-0,20	+	1,38	0,01	0,45
P38647	Hspa9		0,95	0,16	-0,23	+	2,32	0,01	-0,45

GENE		Lrif1 short vs Control				Lrif1 long vs Control			
Uniprot ID	Gene names	Significant (FDR=0.05 S0=0.1)	-Log p-value	q-value	Difference (log2)	Significant (FDR=0.05 S0=0.1)	-Log p-value	q-value	Difference (log2)
G3V004	Calu		0,30	0,55	-0,24	+	1,16	0,02	0,55
Q8VDW0	Ddx39a		1,02	0,13	-0,24	+	1,54	0,03	-0,30
P63330	Ppp2ca		1,61	0,06	-0,25	+	2,96	0,00	-0,49
E9Q8F0	Rbm39		1,08	0,11	-0,25	+	1,23	0,02	-0,46
P19096	Fasn		0,83	0,17	-0,26	+	1,53	0,02	0,33
P97315	Csrp1		0,68	0,22	-0,26	+	1,58	0,01	-0,70
Q4VBE8	Wdr18	+	1,87	0,03	-0,27		0,06	0,94	0,04
P18760	Cfl1		1,46	0,06	-0,27	+	2,35	0,01	-0,42
Q8K3F7	Tdh		1,04	0,10	-0,28	+	1,37	0,02	-0,38
Q792Z1	Try10		1,36	0,06	-0,29	+	1,01	0,05	-0,38
P52624	Upp1		0,90	0,13	-0,29	+	0,94	0,03	0,59
P80316	Cct5	+	2,08	0,02	-0,30		1,17	0,14	0,18
A0A0A0MQA5	Tuba4a		0,23	0,63	-0,30	+	3,41	0,00	1,41
Q61990	Pcbp2	+	1,56	0,03	-0,32		1,77	0,07	-0,18
P48962	Slc25a4	+	1,45	0,04	-0,33		0,33	0,74	-0,07
A0A075B6B4	Trav6-4	+	1,60	0,03	-0,33	+	1,53	0,01	-0,65
P08249	Mdh2		0,68	0,17	-0,36	+	1,36	0,01	-0,68
P63085	Mapk1		0,48	0,30	-0,36	+	2,05	0,00	-1,46
P80314	Cct2	+	1,76	0,02	-0,38	+	4,59	0,01	-0,27
P60335	Pcbp1	+	1,26	0,04	-0,39		0,56	0,37	-0,17
P63325	Rps10	+	1,51	0,03	-0,40	+	1,65	0,01	-0,38
P17742	Ppia		1,01	0,07	-0,40	+	2,24	0,00	-0,87
Q61024	Asns	+	1,86	0,02	-0,41	+	2,69	0,00	-0,61
P45376	Akr1b1	+	1,70	0,02	-0,41		0,80	0,06	-0,50
P56480	Atp5b	+	1,40	0,03	-0,42	+	4,12	0,00	-0,89
Q03265	Atp5a1	+	3,06	0,00	-0,42	+	3,74	0,00	-0,83
P26443	Glud1	+	2,17	0,01	-0,43	+	3,80	0,00	-1,04
A0A087WS46	Eef1b2	+	1,42	0,03	-0,44		1,46	0,05	0,23
P50247	Ahcy	+	1,83	0,01	-0,45		0,78	0,13	-0,29
Q8K2B3	Sdha	+	1,50	0,02	-0,46	+	1,12	0,02	-0,50
Q9DB20	Atp5o	+	1,46	0,02	-0,46	+	1,83	0,00	-0,84
Q9D8W5	Psmd12		0,84	0,09	-0,47	+	1,52	0,01	-0,98
P19324	Serpinh1	+	1,68	0,02	-0,47	+	1,93	0,00	-0,73
Q497W9	Dhx15	+	1,34	0,03	-0,49	+	1,79	0,01	-0,63
P84078	Arf1	+	1,52	0,02	-0,50	+	4,32	0,00	-0,90
A0A0A0MQM0	Eif5a	+	1,79	0,01	-0,50	+	2,14	0,01	-0,46
P29341	Pabpc1	+	2,95	0,00	-0,52	+	2,94	0,00	-0,62
P27773	Pdia3	+	3,35	0,00	-0,52	+	5,09	0,00	-1,09
E9PZF0	Gm20390	+	1,87	0,01	-0,53	+	3,05	0,00	-1,06
Q8BWY3	Etf1	+	1,34	0,02	-0,54	+	2,35	0,00	-0,98
Q9CPY7	Lap3	+	1,94	0,01	-0,54	+	3,38	0,00	-1,16
Q61171	Prdx2	+	1,66	0,01	-0,54	+	2,92	0,00	-1,16
P46935	Nedd4		0,51	0,22	-0,55	+	1,39	0,01	-0,99
P07901	Hsp90aa1	+	1,71	0,01	-0,55		0,62	0,19	-0,29

GENE		Lrif1 short vs Control				Lrif1 long vs Control			
Uniprot ID	Gene names	Significant (FDR=0.05 S0=0.1)	-Log p-value	q-value	Difference (log2)	Significant (FDR=0.05 S0=0.1)	-Log p-value	q-value	Difference (log2)
Q9D0R8	Lsm12	+	1,58	0,01	-0,56	+	1,81	0,01	-0,50
O88569-3	Hnrnpa2b1		0,55	0,19	-0,56	+	1,90	0,00	-1,37
P06151	Ldha	+	1,90	0,01	-0,57	+	1,22	0,01	-1,09
Q8BG32	Psmd11	+	2,42	0,00	-0,58	+	3,06	0,00	-0,77
Q9DCL9	Paics	+	2,08	0,00	-0,59	+	1,71	0,01	-0,57
Q922R8	Pdia6	+	1,79	0,01	-0,60	+	2,57	0,00	-0,92
Q9CZ13	Uqcrc1	+	1,47	0,02	-0,60		0,41	0,50	0,15
A0A0J9YUD8	Hmgb1	+	1,57	0,01	-0,62		0,03	0,96	-0,06
P63038	Hspd1	+	2,61	0,00	-0,62	+	3,09	0,00	-1,02
P62827	Ran	+	3,28	0,00	-0,62	+	3,55	0,00	-0,98
P68040	Gnb2l1	+	3,66	0,00	-0,63	+	4,13	0,00	-1,17
Q61598-2	Gdi2	+	2,15	0,00	-0,63	+	2,40	0,00	-1,06
Q9CXW3	Cacybp	+	1,49	0,01	-0,64	+	2,28	0,00	-1,15
Q64433	Hspe1	+	1,37	0,02	-0,65	+	2,23	0,00	-0,94
P58252	Eef2	+	2,17	0,00	-0,66	+	2,85	0,00	-1,02
Q9CQR2	Rps21	+	3,64	0,00	-0,67	+	1,13	0,01	-1,69
Q7TNC4-2	Luc7l2		0,90	0,06	-0,68	+	0,95	0,03	-0,66
P40142	Tkt	+	2,00	0,00	-0,69	+	3,37	0,00	-1,12
P10126	Eef1a1	+	3,19	0,00	-0,70	+	3,63	0,00	-0,88
Q61937	Npm1	+	1,63	0,01	-0,70		0,69	0,10	-0,46
A0A0U1RNT6	Mat2a	+	2,24	0,00	-0,71		0,89	0,08	-0,33
P17751	Tpi1	+	2,81	0,00	-0,71	+	2,59	0,00	-1,08
P63028	Tpt1	+	2,48	0,00	-0,72	+	2,75	0,00	-1,09
A0A1D5RLS2	Nudt21	+	1,85	0,00	-0,73	+	2,48	0,00	-0,97
A6ZI44	Aldoa	+	2,31	0,00	-0,73	+	2,47	0,00	-1,07
Q62446	Fkbp3	+	1,47	0,01	-0,75	+	2,23	0,00	-1,28
P17182	Eno1	+	2,81	0,00	-0,75	+	2,56	0,00	-1,12
Q8K274	Fn3krp		0,83	0,06	-0,76	+	1,08	0,01	-0,92
Q5F2E7	Nufip2	+	1,68	0,01	-0,76	+	1,66	0,01	-0,77
P30681	Hmgb2	+	1,33	0,02	-0,77		0,42	0,19	-1,54
P14685	Psmd3	+	1,57	0,01	-0,79	+	2,08	0,00	-1,14
P11440	Cdk1		0,48	0,21	-0,79	+	2,25	0,00	-0,64
S4R1W1	Gm3839	+	3,35	0,00	-0,80	+	2,67	0,00	-1,00
B1AXW5	Prdx1	+	4,03	0,00	-0,80	+	2,67	0,00	-1,19
P57784	Snrpa1	+	2,26	0,00	-0,82	+	2,57	0,00	-1,04
Q3U2G2	Hspa4	+	0,98	0,03	-0,82	+	0,82	0,03	-0,95
Q9D0M3	Cyc1	+	1,01	0,03	-0,83		0,81	0,06	-0,47
E9Q5Q0	Atxn2l	+	3,02	0,00	-0,83	+	3,32	0,00	-0,84
Q3UL36	Arglu1	+	2,05	0,00	-0,85	+	2,25	0,00	-1,04
A0A0N4SV32	Serbp1	+	2,69	0,00	-0,86	+	2,59	0,00	-0,96
Q9CPN9	22100 10C04Rik	+	1,48	0,01	-0,86	+	1,12	0,04	-0,39
P47738	Aldh2	+	0,87	0,05	-0,87	+	1,00	0,03	-0,56
O89086	Rbm3	+	1,26	0,02	-0,88	+	1,48	0,01	-0,94

GENE		Lrif1 short vs Control				Lrif1 long vs Control			
Uniprot ID	**Gene names**	**Significant (FDR=0.05 S0=0.1)**	**-Log p-value**	**q-value**	**Difference (log2)**	**Significant (FDR=0.05 S0=0.1)**	**-Log p-value**	**q-value**	**Difference (log2)**
Q60817	Naca	+	1,44	0,01	-0,88	+	2,72	0,00	-1,52
G3UXT7	Fus	+	1,60	0,01	-0,88	+	1,63	0,01	-0,80
Q9CZN7-2	Shmt2	+	1,62	0,01	-0,89	+	4,57	0,00	-1,47
Q9CZU6	Cs	+	3,86	0,00	-0,89	+	2,29	0,00	-1,28
P14206	Rpsa	+	4,14	0,00	-0,89	+	3,02	0,00	-1,31
Q60864	Stip1	+	1,95	0,00	-0,89	+	2,70	0,00	-1,39
Q5EBP8	Hnrnpa1	+	0,88	0,05	-0,89	+	1,27	0,01	-1,08
P63260	Actg1	+	1,78	0,00	-0,90	+	3,87	0,00	-1,46
P24369	Ppib	+	2,14	0,00	-0,90	+	2,22	0,00	-1,42
P61982	Ywhag	+	2,88	0,00	-0,91	+	3,38	0,00	-1,08
Q9DBJ1	Pgam1	+	2,58	0,00	-0,92	+	2,29	0,00	-1,17
P54823	Ddx6		0,47	0,22	-0,94	+	1,09	0,03	-0,53
Q5XJY5	Arcn1	+	1,06	0,02	-0,97	+	1,53	0,01	0,66
Q8VIJ6	Sfpq	+	1,96	0,00	-0,99	+	2,54	0,00	-0,95
Q8BK67	Rcc2	+	2,37	0,00	-0,99	+	2,05	0,00	-1,26
A2AL12	Hnrnpa3	+	2,96	0,00	-1,01	+	2,04	0,00	-1,06
Q8QZY1	Eif3l	+	1,08	0,02	-1,01	+	1,31	0,01	-1,21
P07356	Anxa2	+	2,71	0,00	-1,07	+	3,19	0,00	-1,69
Q80X90	Flnb	+	3,77	0,00	-1,07	+	2,87	0,00	-1,13
Q99K48	Nono	+	1,62	0,00	-1,10	+	2,52	0,00	-0,64
B1AZS9	Prdx4	+	1,92	0,00	-1,11	+	3,78	0,00	-1,39
D3Z0Y2	Prdx6	+	1,56	0,01	-1,12	+	1,88	0,00	-1,59
Q9CWJ9	Atic	+	1,01	0,03	-1,17	+	0,96	0,02	-0,89
Q61792	Lasp1	+	2,95	0,00	-1,22	+	3,46	0,00	-1,34
Q8BGJ5	Ptbp1	+	2,65	0,00	-1,26	+	2,61	0,00	-1,52
Q99KI0	Aco2	+	2,10	0,00	-1,31	+	2,58	0,00	-1,17
A0A1L1SV25	Actn4	+	1,60	0,00	-1,35	+	3,69	0,00	-2,21
Q9JMD0-4	Znf207	+	1,09	0,02	-1,36	+	2,36	0,00	-1,95
O35685	Nudc	+	3,71	0,00	-1,65	+	3,99	0,00	-1,88
A2BE93	Set	+	1,46	0,00	-1,69		0,08	0,90	-0,15
P10852	Slc3a2	+	3,40	0,00	-1,79	+	2,95	0,00	-2,38
Q99LX0	Park7	+	2,89	0,00	-1,79		0,15	0,85	-0,07
P14733	Lmnb1	+	1,21	0,01	-1,80	+	1,89	0,00	-1,83
P26043	Rdx	+	2,22	0,00	-2,29	+	2,44	0,00	-2,36
P55821	Stmn2	+	3,06	0,00	-2,35	+	3,19	0,00	-3,10
F8WIT2	Anxa6	+	4,59	0,00	-2,55	+	5,81	0,00	-2,98
Q07076	Anxa7	+	6,72	0,00	-2,80	+	3,53	0,00	-2,65
Q6PIX5-2	Rhbdf1		0,66	0,07	-2,86	+	2,15	0,00	-1,20
P21107-2	Tpm3	+	5,50	0,00	-2,97	+	4,50	0,00	-3,43

Suppl. Table 3. Primers used for qRT-PCR.

Primer name	Primer sequence 5'->3'
mβ-actin_RT_F	GGCTGTATTCCCCTCCATCG
mβ-actin_RT_R	CCAGTTGGTAACAATGCCATGT
mLRIF1l+s qPCR F	AAGATGCAAACATTGTGGTG
mLRIF1l+s qPCR R	CCATCTTCATGGTTTCCGC
Smchd1 ex44_F	AAGCCCTTTGGAAATCCAGT
Smchd1 ex46_R	TGGGGCAGTGTGTGATTTTA
mDnmt3b_RT_Ex16-17_F	GGAAGAATTTGAGCCACCCA
mDnmt3b_RT_Ex18_R	GACTTCGGAGGCAATGTACTT
endo-mOct4-F	TAGGTGAGCCGTCTTTCCAC
endo-mOct4-R	GCTTAGCCAGGTTCGAGGAT
endo-mSox2-F	AGGGCTGGGAGAAAGAAGAG
endo-mSox2-R	CCGCGATTGTTGTGATTAGT
endo-mNanog-F	CTCAAGTCCTGAGGCTGACA
endo-mNanog-R	TGAAACCTGTCCTTGAGTGC
mTrim28-1241-F2	CTGGTACGAACTCCACAGGT
mTrim28-1439-R2	CCACTTACCTCTCCCTCACC
mDux_1 F	ACTTCTAGCCCCAGCGACTC
mDux_1 R	CCATGCTGCCAGGATTTCTA
Gm21761 F	GATCCCTGAGGGTAAGTCCTCC
Gm21761 R	TGCTTCCTATCCAGCTCTTGAGG
Usp17lb F	CTTCCCAGAAGATCCAGCC
Usp17lb R	CTGTGCTTTCCATTGGCAG
Gm2016 F	TACTCACCAGGTCAATGCAG
Gm2016 R	AGGAAGGTGTAGTCTCCCT
Tmem92 F	GTAAGCTTCAATGAGACTGCA
Tmem92 R	GCAGCATTCCTTGACACAG
mZscan4e-358-F	TTGAAGCCTCCTGTCATGGT
mZscan4e-515-R	TGTGTGGTGTCTACTGGCAT

Suppl. Table 4. Information about batch effects due to separate knock-down experiments and re-sequencing of siDnmt3b_1 sample.

Sample Name	Experiment ID	Sequencing run ID
siNT_1	E1	SR1
siNT_2	E2	SR1
siNT_3	E3	SR1
siLrif1_1	E1	SR1
siLrif1_2	E2	SR1
siLrif1_3	E3	SR1
siSmchd1_1	E1	SR1
siSmchd1_2	E2	SR1
siSmchd1_3	E3	SR1
siDnmt3b_1	E1	SR2
siDnmt3b_2	E2	SR1
siDnmt3b_3	E3	SR1

Suppl. Table 5. Cloning primers for creating mPVL and m1 mutants in Lrif1l/s ORF.

Mutant Name	Insert	Forward primer (5'->3')	Reverse primer (5'->3')
Lrif1l mPVL	Insert 1	CATGGTCCTGCTGGAGTTCGTG	GATGGTCAGGAATTCGAGTTTCA-CAGTCTCTCAAATCTTTAGTGAG
	Insert 2	CTCACTAAAGATTTGAGAGACTGT-GAAACTCGAATTCCTGACCATC	ACAGGGATTTCTTGTCTCCC
	Insert 1 + Insert 2	CATGGTCCTGCTGGAGTTCGTG	ACAGGGATTTCTTGTCTCCC
Lrif1l m1	Insert 1	CATGGTCCTGCTGGAGTTCGTG	CTTTTTCTCTTAAAATTTGCT-CAGCTTCTCTTATTTTTTCATCTCTGATG
	Insert 2	CATCAGAGATGAAAAAATAA-GAGAAGCTGAGCAAATTTTAA-GAGAAAAAG	ACAGGGATTTCTTGTCTCCC
	Insert 1 + Insert 2	CATGGTCCTGCTGGAGTTCGTG	ACAGGGATTTCTTGTCTCCC
Lrif1s mPVL	Insert 1	CATGGTCCTGCTGGAGTTCGTG	GATGGTCAGGAATTCGAGTTTCA-CAGTCTCTCAAATCTTTAGTGAG
	Insert 2	CTCACTAAAGATTTGAGAGACTGT-GAAACTCGAATTCCTGACCATC	ACAGGGATTTCTTGTCTCCC
	Insert 1 + Insert 2	CATGGTCCTGCTGGAGTTCGTG	ACAGGGATTTCTTGTCTCCC
Lrif1s m1	Insert 1	CATGGTCCTGCTGGAGTTCGTG	CTTTTTCTCTTAAAATTTGCT-CAGCTTCTCTTATTTTTTCATCTCTGATG
	Insert 2	CATCAGAGATGAAAAAATAA-GAGAAGCTGAGCAAATTTTAA-GAGAAAAAG	ACAGGGATTTCTTGTCTCCC
	Insert 1 + Insert 2	CATGGTCCTGCTGGAGTTCGTG	ACAGGGATTTCTTGTCTCCC